

## Lectures

# Thermal Cracking of a Concrete Arch Dam

M. Goldgruber, R. Lampert

# Thermal Cracking of a Concrete Arch Dam

Goldgruber M.<sup>1</sup>, Lampert R.<sup>1</sup>

<sup>1</sup> DYNARDO Austria GmbH, Vienna, AUSTRIA

E-mail: [markus.goldgruber@dynardo.at](mailto:markus.goldgruber@dynardo.at)

**ABSTRACT:** This benchmark workshop on numerical analysis of dams deals with seasonal temperature variations with high gradients and its effects on an arch dam. Linear and nonlinear analyses, regarding the material model, are performed for a 2-year period of a cold year followed by a warm year. In the nonlinear case, the damaged plasticity model for concrete according to Menetrey and Willam is used. The nonlinear analysis of the arch dam shows some significant differences compared to the linear analysis, which are directly attributable to the nonlinear effects of relaxation. Rearrangements of stresses lead to a change in the expected crack pattern, decrease of the minimum displacements and an increase of the maximum displacements. Nevertheless, for investigations regarding possible areas subjected to cracks, linear analysis can deliver a first guess, but cannot predict crack directions and extent. It can be concluded, that for such investigations of a dam structure, nonlinear analyses are prerequisite. Especially in the case of preliminary studies of dam structures subjected to high temperature gradients, because foreknowledge leads to decisions regarding necessary structural measures in the planning phase.

## 1 Introduction and problem description

The focus of this benchmark theme [1] is the analysis and verification of concrete cracking subjected to seasonal temperature variations of an arch dam. The contributors are intended to use different nonlinear material models, meshes, temperature analyses types (steady-state or transient) and boundary/contact formulations. The geometry, standard material parameters, loads and temperatures are well defined by the formulators in [1]. Specific properties for nonlinear materials are intended to be chosen by the formulators, as well as contact formulations for the interface between the dam body and the rock foundations.

The formulators provided geometry files in STEP- and ACIS-format. The model in these files are already split in two parts in general, the rock foundation and dam body. The dam body includes a footing at the orographic left side and the spillway on the orographic right side.

The concrete arch dam has a height of approx. 40 meters and a crest length of 170 meters. The crest has a radius of 110 meters. The boundaries of the rock measure approx. 193 meters times 225 meters, with a maximum height of 60 meters.

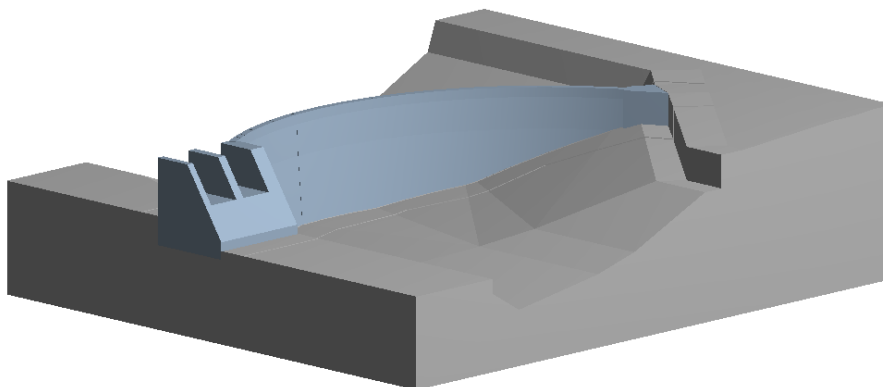


Figure 1: Dam model (left) and reinforcement (right) in the dam body.

According to the formulators the dam also has 3 reinforcement layers.

- Upstream: 1 layer
  - Horizontal and vertical reinforcement bars with 25mm in diameter and a spacing of 300mm, with a concrete cover of 100mm.
- Downstream: 2 layers
  - 1<sup>st</sup> layer: Horizontal and vertical reinforcement bars with 25mm in diameter and a spacing of 300mm, with a concrete cover of 100mm.
  - 2<sup>nd</sup> layer: Vertical reinforcement bars with 25mm in diameter and a spacing of 300mm, with a concrete cover of 200mm.

## 2 The finite element model

Based on the geometry provided, the mesh of the finite element model is prepared using ANSYS 18.1 [7]. Dependent on the analysis, transient temperature analysis and mechanical analysis, the mesh is slightly different. Table 1 summarizes the mesh properties of the parts and the different analysis types. Figure 2 depicts the mesh of the rock foundation, the arch dam body and the reinforcement.

Table 1: Summary of the mesh of transient thermal analysis and the mechanical analysis.

	<b>Transient thermal analysis</b>	<b>Mechanical analysis</b>
Formulation	8 Node linear brick	8 Node linear brick
Nodes	67400	470000
Elements	65500	475000
Characteristic size of the Dam/Reinforcement mesh	1.0 m	0.5 m
Characteristic size of the Rock foundation mesh	4.0 m – 7.0 m	1.00 m – 8.0 m

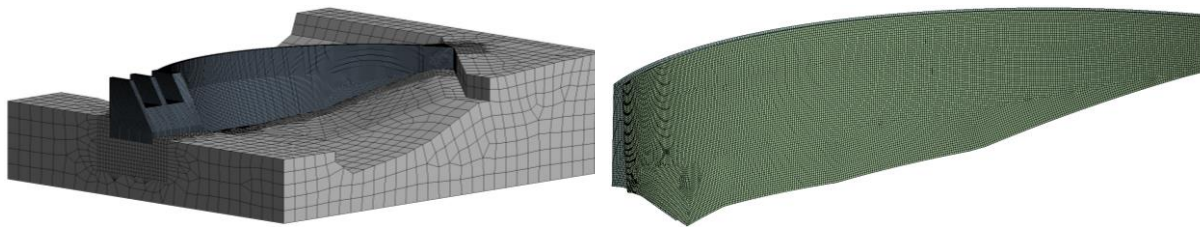


Figure 2: Mesh of the rock foundation, the arch dam body and the reinforcement.

The reinforcement shell elements have a thickness of 1.64 mm, which corresponds to the area of the reinforcement per meter ( $A_{\text{reinf}}/a = 490.9 \text{ mm}^2/300 \text{ mm} = 1.64 \text{ mm}$ ) defined by the formulators in [1]. The shell elements are embedded and coupled to the concrete arch dam. Due to the fact, that such couplings are done on a nodal basis, care is taken, that the nodes of the elements of the dam and the reinforcement are approx. at the same location.

### 2.1 Material properties

Overall 3 different materials (concrete, reinforcement steel, rock) are defined by the formulators in [1]. Except for the concrete no additional material properties must be defined.

For the simulation of the cracking in the arch dam, the constitutive model for concrete plasticity according to Menetrey-Willam [5] is used, which is based on Willam-Warnke [6] yield surface. Hence, additional parameters must be defined. Table 3 summarizes all parameters, which are necessary for the definition of the concrete softening in compression and tension. Figure 3 illustrates the softening curves and their parameters. The area specific fracture energy (area under the softening curve) has been derived from a former project at Dynardo GmbH in

cooperation with a customer performing physical model tests on precast concrete walls. The numerical model for the test setup has been calibrated with the help of ANSYS *optiSlang*<sup>®</sup> [8] resulting in realistic crack patterns and fitting load-displacement curves.

Table 2: Standard concrete material properties [1].

Property	Value	Unit
Youngs-modulus	33	GPa
Poisson's ratio	0.2	-
Density	2300	kg/m <sup>3</sup>
Compressive strength	38	MPa
Tensile strength	2.9	MPa
Thermal expansion	1.00E-05	K <sup>-1</sup>
Thermal conductivity	2	W/(m*K)
Stress/strain free temperature	4	°C
Specific heat capacity	900	J/(kg*K)

Table 3: Additional specific concrete material properties for the use of the Menetrey-Willam concrete plasticity material model with exponential softening.

Property	Value	Unit
Uniaxial tensile strength	2.9	MPa
Biaxial compressive strength	38	MPa
Uniaxial compressive strength	31.7	MPa
Dilation angle	15	°
Relative stress level $\Omega_{cu}$ at $\kappa_u$	0.85	-
Plastic strain at uni-axial compressive strength $\kappa_{cm}$	0.00124	-
Plastic strain defining start of exponential softening $\kappa_{cu}$	0.0027	-
Relative stress level at start of hardening $\Omega_{ci}$	0.4	-
Residual relative stress level in compression $\Omega_{cr}$	0.2	-
Residual relative stress level in tension $\Omega_{tr}$	0.01	-
Area specific fracture energy	200	Nm/m <sup>2</sup>

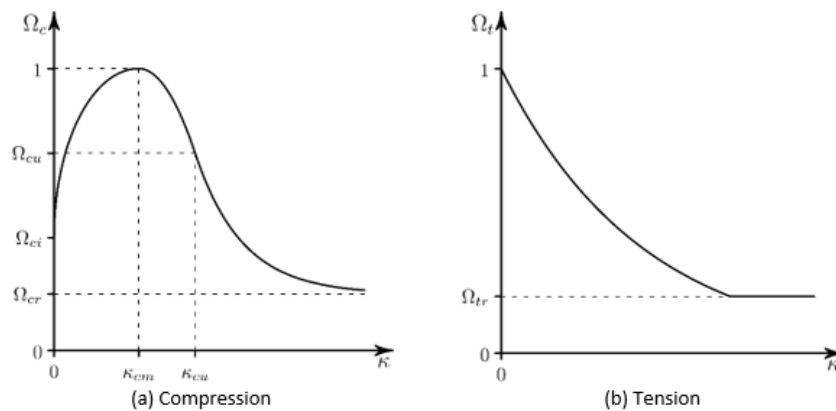


Figure 3: Exponential softening in compression and tension from the ANSYS Manual [7].

The reinforcement material properties for the thermal and mechanical analysis are summarized in Table 4. The material model for the reinforcement is chosen to be nonlinear with multilinear

isotropic hardening as depicted in Figure 4. The additional reinforcement with only vertical bars on the downstream side has orthotropic material properties with reduced Youngs-modulus and shear modulus in horizontal direction by a factor of 1000.

Table 4: Reinforcement material properties [1].

Property	Value	Unit
Youngs-modulus	200	GPa
Poisson's ratio	0.3	-
Density	7800	kg/m <sup>3</sup>
Yield stress	360	MPa
Ultimate strength	600	MPa
Ultimate strain	0.15	-
Thermal expansion	1.00E-05	K <sup>-1</sup>
Thermal conductivity	39	W/(m*K)
Stress/strain free temperature	4	°C
Specific heat capacity	450	J/(kg*K)

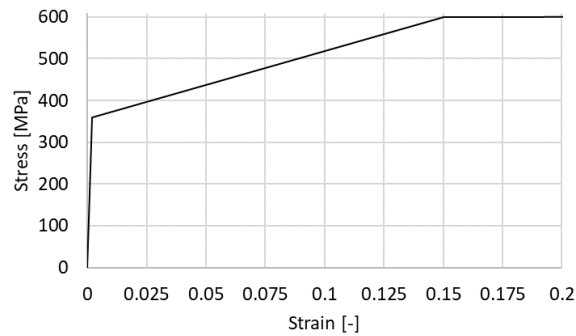


Figure 4: Stress-strain relationship for the nonlinear reinforcement.

The rock material properties for the thermal and mechanical analysis are summarized in Table 5. The material model for the rock is completely linear elastic and isotropic.

Table 5: Rock material properties.

Property	Value	Unit
Youngs-modulus	40	GPa
Poisson's ratio	0.15	-
Density	2700	kg/m <sup>3</sup>
Thermal expansion	1.00E-05	K <sup>-1</sup>
Thermal conductivity	3	W/(m*K)
Stress/strain free temperature	4	°C
Specific heat capacity	850	J/(kg*K)

## 2.2 Thermal conditions and loads

In the thermal analysis, the temperatures are defined as ambient air temperatures, hence convective heat transfer coefficients are necessary. The recommended parameters according to [1] are summarized in Table 6.

Table 6: Convective heat transfer coefficients [1].

	<b>Convective heat coefficient W/(m<sup>2</sup> K)</b>	<b>Unit</b>
Downstream surface of the arch dam – air	4	The downstream surface should be considered to have lower convective heat coefficient compared to other concrete surfaces. (the reason is that there is usually some heat insulating material installed on the downstream surface on dams in Sweden)
Concrete – air	13	For all surfaces exposed to air, except the downstream surface of the arch dam.
Concrete – water	500	
Concrete - rock	1000	
Rock – air	13	
Rock – water	500	

A transient thermal analysis is performed to calculate the temperature distribution in the rock foundation and arch dam body. The monthly temperatures for a cold and warm year are provided in [1]. Two whole years are simulated for the varying temperature starting with a cold year followed by a warm year. The starting month is June which has a temperature close to the strain free temperature of the concrete and rock according to Table 2 and Table 5 (However, the simulation starts with April, because for the vice versa case with a warm year starting, the strain free temperature is close in April and the comparisons might be easier). Figure 5 illustrates the temperature variation, applied to the transient thermal simulation, over 2 years.

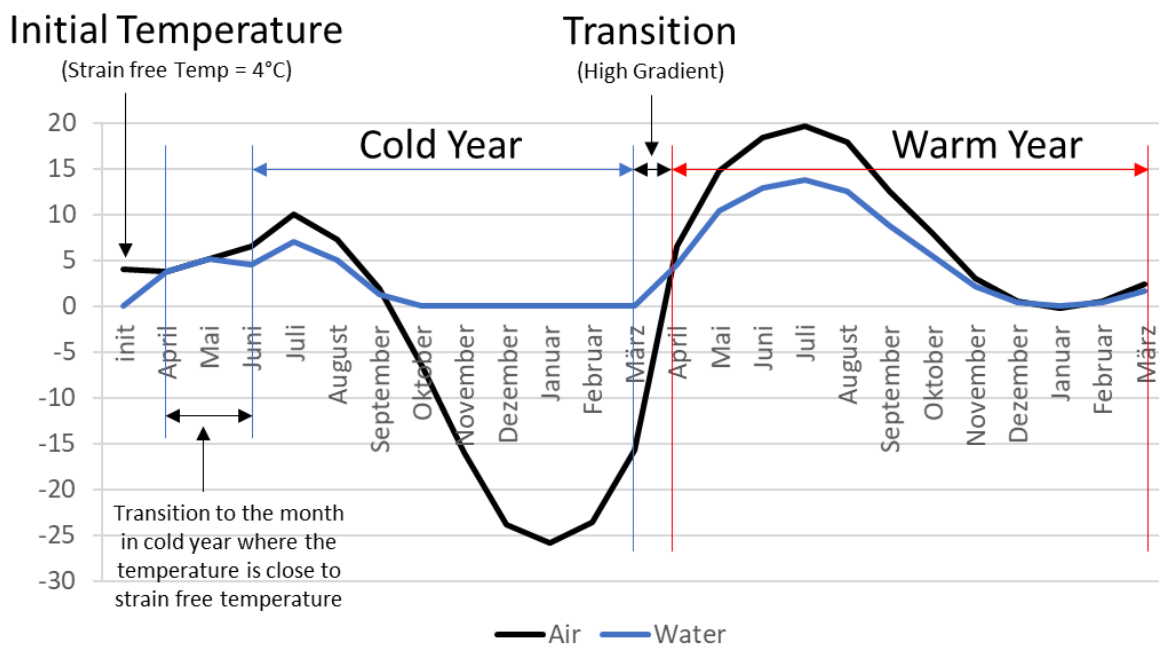


Figure 5: Temperature variation applied to the transient thermal simulation; Starting with a cold year, followed by a warm year.

### 2.3 Mechanical loads

The mechanical loads on the model are the deadweight of the arch dam, the hydrostatic load for full reservoir conditions (water level = crest level) and the contraction/expansion loads coming from thermal strain due to the 2-year period of temperature variation computed in the subsequent transient thermal analysis. Construction steps and the gravity on the rock mass are neglected.

### 2.4 Boundary conditions and contact definitions

The boundary conditions are defined at rock foundation boundaries and the orographic right end of the spillway. The displacements normal to these boundaries are prohibited. Hence, only tangential displacements are allowed.

The contact definitions between the arch dam and the foundation interface are defined to follow a “rough” formulation. Such contacts prohibit relative displacement, but allow for openings. This assumption is considered as a post-cracked condition, therefore, no tensile stresses, only shear stresses are transferred at the interface of these two bodies. The left footing and the spillway are also not connected to the foundation on the upstream side (post-cracked condition). In case of the linear analysis the rough contact is still active.

### 2.5 Analysis types

Overall three analyses are performed with the parameters and assumptions described in the former sections:

1. Transient thermal analysis over a period of 2 years. Cold year – Warm year.
2. Linear static analysis (only material linear, contact definition as described in section 2.4 still active)
3. Nonlinear static analysis over a period of 2 years. Cold year – Warm year.

For both, the linear and nonlinear analysis, the applied load steps are the same:

1. Deadweight (Gravity load on the dam)
2. Hydrostatic water load
3. Temperature variation from the preceding transient thermal analysis

## 3 Results

### 3.1 Results of the thermal analysis

Figure 6 shows the maximum temperature, which occurs in July and the minimum temperature, which occurs in January from the transient thermal analysis.

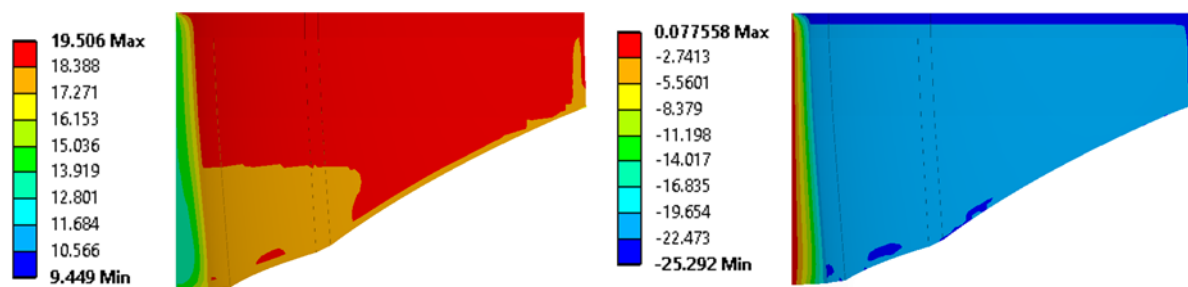


Figure 6: Temperature distributions in the dam body in July (left) and January (right).

### 3.2 Results of the linear mechanical analysis

Figure 7 and Figure 8 show the maximum resultant displacement at the dam body of the linear analysis for the coldest month January and the warmest month July, respectively.

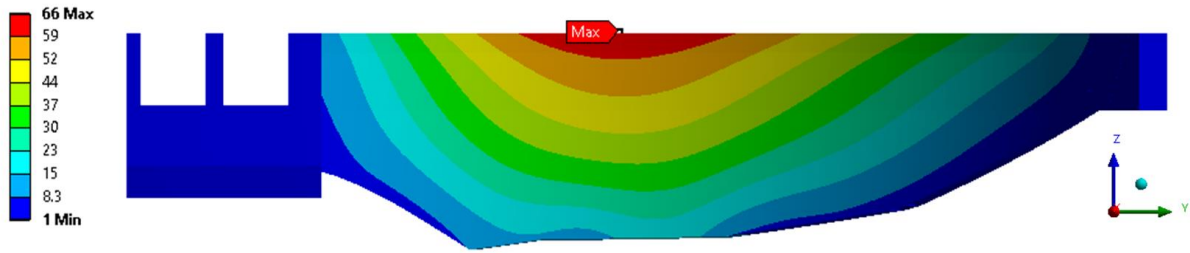


Figure 7: Contour plot of the x displacement [mm] in January (coldest month).

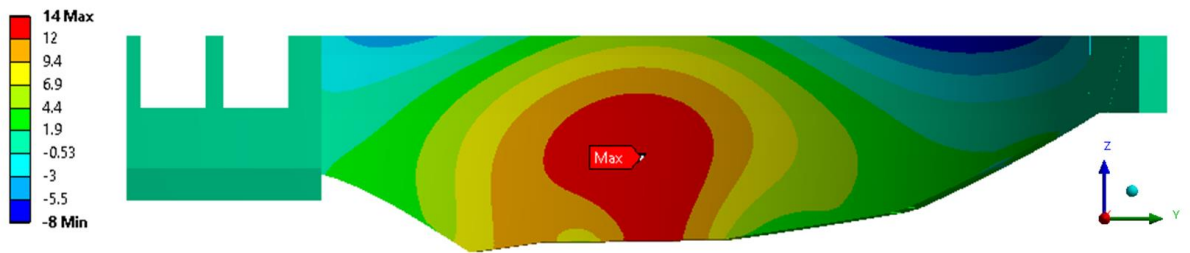


Figure 8: Contour plot of the x displacement [mm] in July (warmest month).

Figure 9 shows the maximum principal stresses at the dam body of the linear analysis over all time instants. Red areas are illustrating the areas which are exceeding the tensile strength of 2.9 MPa, i.e. the areas that may be subjected to cracking.

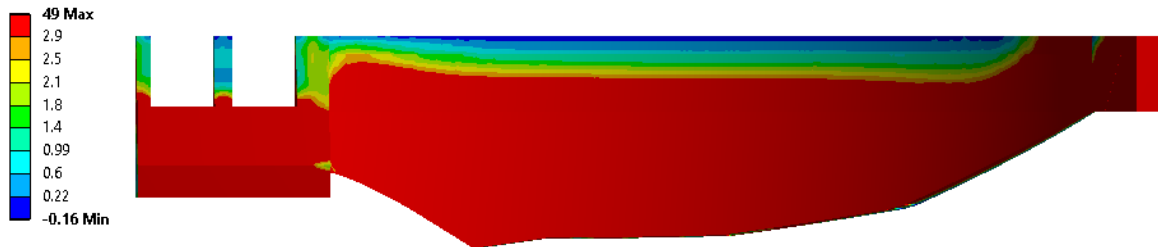


Figure 9: Contour plot of the maximum principal stresses [MPa] – envelope over time.

Figure 10 illustrates the vector components of the principal stresses. Red lines indicate tensile stress components, which highlight possible areas that may be subjected to cracking.

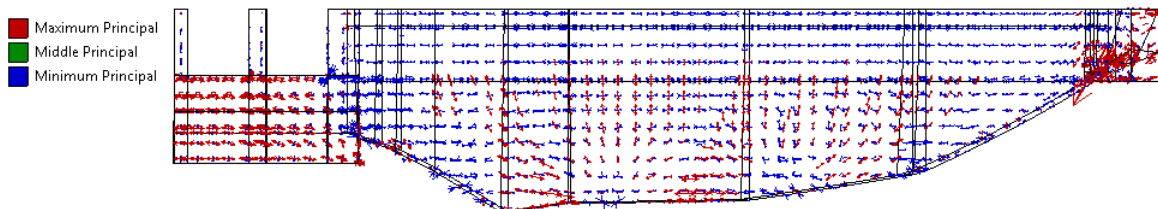


Figure 10: Vector plot of the principal stress – envelope over time.



### 3.3 Results of the nonlinear mechanical analysis

Figure 11 and Figure 12 show the maximum resultant displacement at the dam body of the nonlinear analysis for the coldest month January and the warmest month July, respectively.

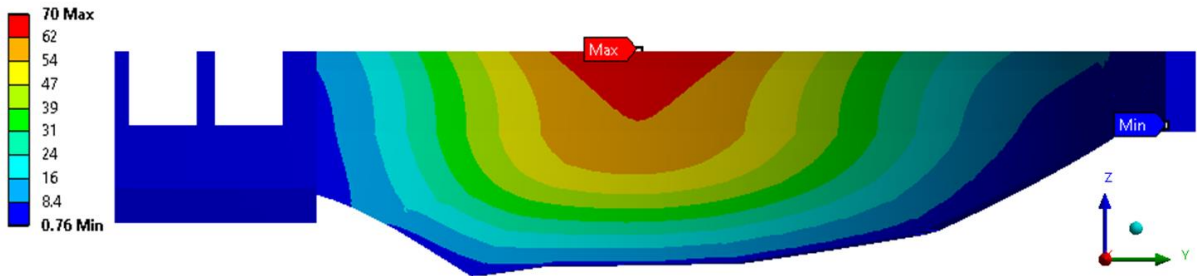


Figure 11: Contour plot of the x displacement [mm] in January (coldest month).

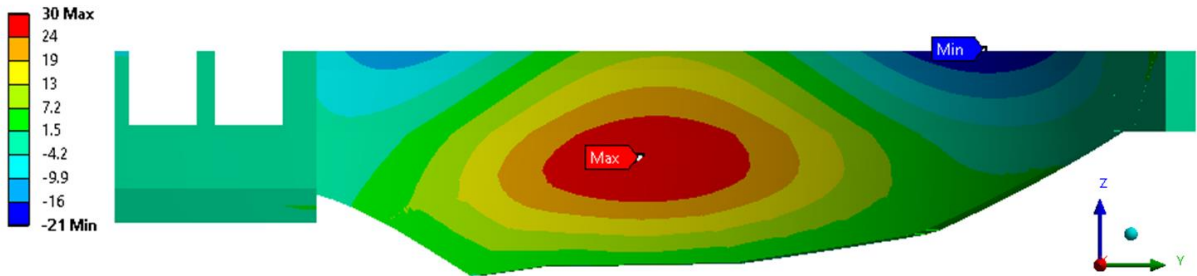


Figure 12: Contour plot of the x displacement [mm] in July (warmest month).

Figure 13 shows the equivalent plastic strain at the end of the simulation (2 years, cold-warm year) at the dam body of the nonlinear analysis on the downstream side. Red areas are indicating areas that are subjected to cracks. Therefore, the maximum allowed plastic strain is chosen to be  $\epsilon_p > 0.3\%$ . Figure 14 shows the same results for the upstream side of the dam body.

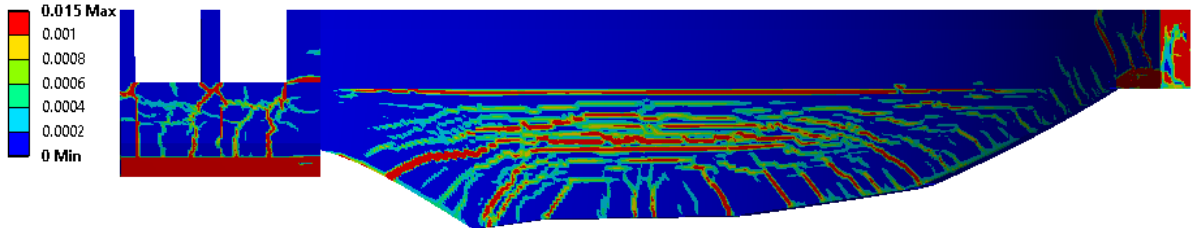


Figure 13: Downstream view of the equivalent plastic strains at the end of the simulation (2 Years, Cold-Warm Year); Red areas are subjected to cracks ( $\epsilon_p > 0.3\%$  plastic strain).



Figure 14: Upstream view of equivalent plastic strains at the end of the simulation (2 Years, Cold-Warm Year); Red areas are subjected to cracks ( $\epsilon_p > 0.3\%$  plastic strain). Comparison between the linear and nonlinear results

### 3.4 Comparison of the linear and nonlinear mechanical analysis

In this section, the linear and nonlinear displacements along three different lines of the dam body are compared. All displacements are shown in x-direction (upstream to downstream).

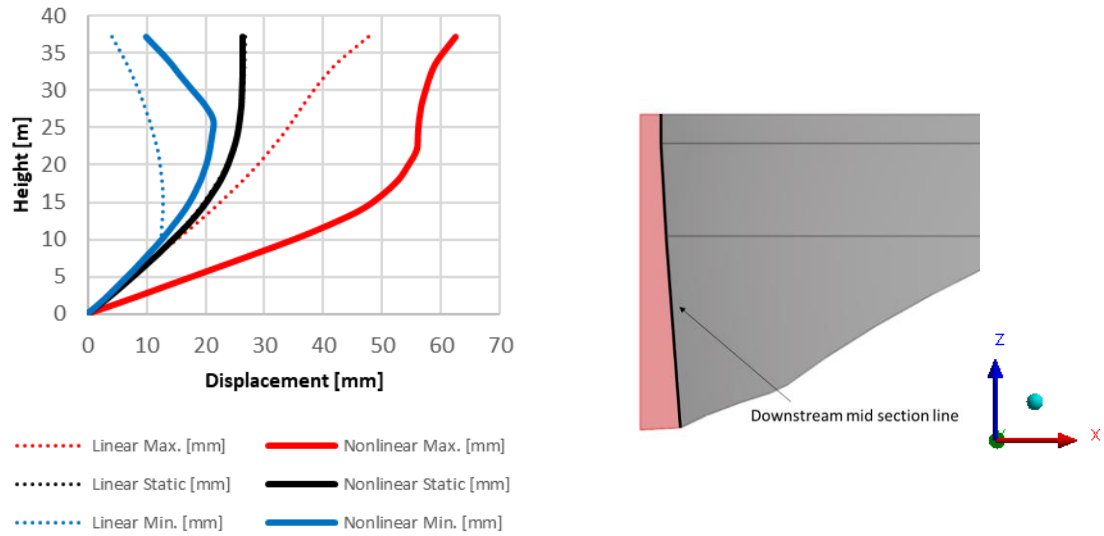


Figure 15: Comparison between linear and nonlinear displacements envelopes over the 2-year period at the mid-section on the downstream side of the dam in x-direction. Adjusted to be zero at the base.

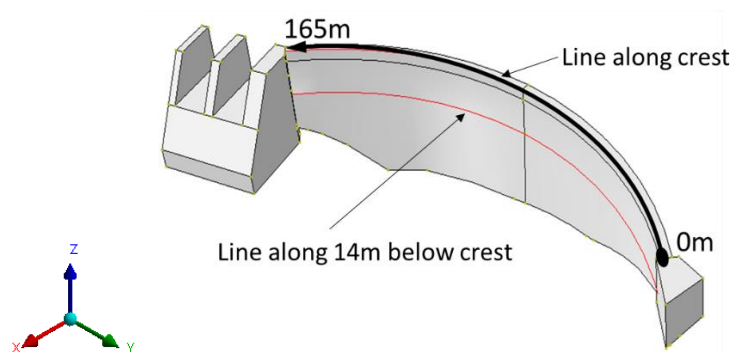
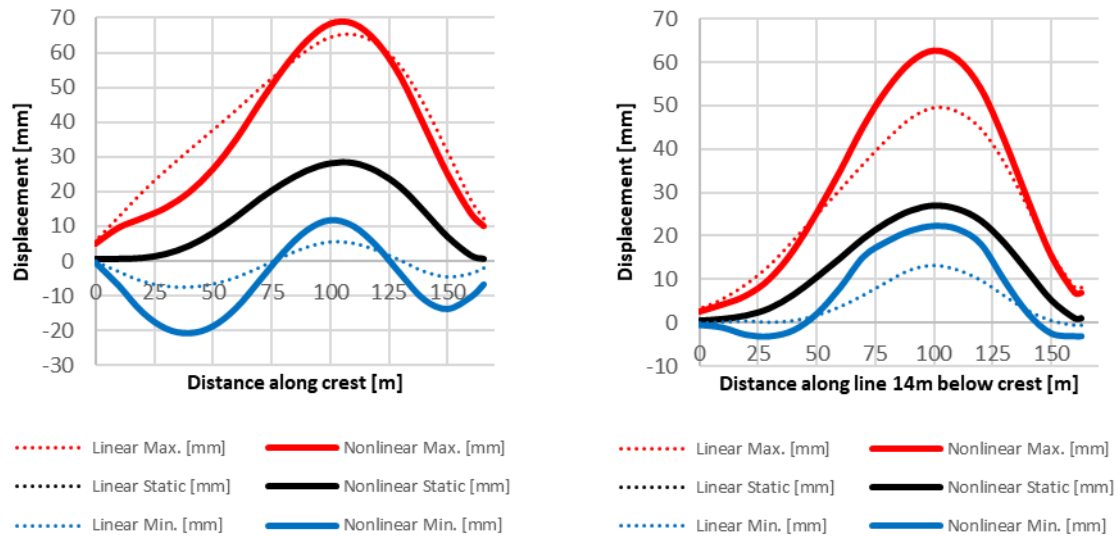


Figure 16: Comparison between linear and nonlinear displacements envelopes over the 2-year period along the crest and along a line 14m below the crest in x-direction.

## 4 Conclusion

The nonlinear analysis of the arch dam in this benchmark workshop shows some significant differences to the linear analysis. The displacements show variations at the crest and at mid height up to 10 mm for the minimum and maximum envelope over the whole period of 2 years. These differences are directly attributable to the crack pattern at the downstream surface of the arch dam, which are leading to a relaxation of the structure. This effect leads to a decrease of the minimum displacements and an increase of the maximum displacements.

Comparing the linear principal stress vector plot and the crack pattern in the plastic strain plot reveals some similarities. Some areas with maximum principal vectors coincide with cracked areas from the nonlinear analysis, especially at the left footing and areas near the downstream bottom line. Hence, for investigations regarding areas subjected to cracks, linear analysis can deliver a first guess, but cannot account for structural relaxation and rearrangements of stresses, accompanying crack direction and extent. For instance, the contour plot of the maximum principal stresses of the linear analysis shows areas where the maximum allowed tensile stress of 2.9 MPa is exceeded. Hence, the conclusion out of a linear analysis would be, that the whole downstream side must be subjected to cracks, which cannot be the case from a practical point of view.

It can be concluded, that for investigations of a dam structure, regarding areas subjected to cracks, nonlinear analyses are prerequisite. Especially in the case of preliminary studies of dam structures subjected to high temperature gradients, because the foreknowledge leads to decisions, whether reinforcement is necessary in some areas or even not. It should be kept in mind that the temperature variation plays a non-negligible role, especially the effects of a cold year followed by a warm year, or vice versa. Furthermore, Additional cycles of annual variations might be necessary to deliver elaborated results in some cases.

## 5 References

- [1] Malm R., Gasch T., Ekström T., Fu C. (2017). Theme A - Thermal cracking of a concrete arch dam. 14th International Benchmark Workshop on Numerical Analysis of Dams, Stockholm
- [2] Léger P., Seydou S. (2009) Seasonal Thermal Displacements of Gravity Dams Located in Northern Regions. *Journal of Performance of Constructed Facilities*, ASCE, 23, pp. 166-174
- [3] Malm R., Ansell A. (2011) Cracking of Concrete Buttress Dam Due to Seasonal Temperature Variation. *ACI Mechanical Journal*, 108-S02, pp. 13-22
- [4] Malm R. (2016) Guideline for FE analyses of concrete dams. Energiforsk report 2016:270. Energiforsk AB. Available for download from:  
<https://energiforskmedia.blob.core.windows.net/media/21143/guideline-for-fe-analyses-of-concrete-dams-energiforskrappport-2016-270.pdf>
- [5] Menetrey, P. (1994) Numerical Analysis of Punching Failure in Reinforced Concrete Structures. Diss. Ecole Polytechnique Federale de Lausanne, Lausanne. Infoscience. Web.
- [6] Willam, K. J., Warnke E. P. (1975) "Constitutive Models for the Triaxial Behavior of Concrete." Seminar on Concrete Structures Subjected to Triaxial Stresses. International Association for Bridge and Structural Engineering. 19: 1-30.
- [7] ANSYS, Inc. (2017) ANSYS Documentation, ANSYS, Inc., Canonsburg, PA 15317  
<http://www.ansys.com>
- [8] Dynardo GmbH (2017). Methods for multi-disciplinary optimization and robustness analysis. Dynardo GmbH, Weimar, [www.dynardo.de](http://www.dynardo.de)